Doi: 10.1007/s11589-010-0740-8

Seismic interferometry and estimation of the Green's function using Gaussian beams*

Robert L. Nowack ♣
Department of Earth and Atmospheric Sciences, *Purdue University*, *West Lafayette*, *IN* 47907, *USA*

Abstract This study investigates seismic interferometry in which the Green's function is estimated between two receivers by cross-correlation and integration over sources. For smoothly varying source strengths, the dominant contributions of the correlation integral come from the stationary phase directions in the forward and backward directions from the alignment of the two receivers. Gaussian beams can be used to evaluate the correlation integral and concentrate the amplitudes in a vicinity of the stationary phase regions instead of completely relying on phase interference. Several numerical examples are shown to illustrate how this process works. The use of Gaussian beams for the evaluation of the correlation integral results in stable estimates, and also provides physical insight into the estimation of the Green's function based on seismic interferometry.

Key words: **seismic interferometry; Gaussian beams; Green's function**
CLC number: P3195.01 **Document code**: A

1 Introduction

Seismic interferometry can be used to determine the Green's function between two receivers as if a source were located at one receiver and recorded at the other receiver utilizing distant seismic energy. The development and many applications of seismic interferometry have been described in recent literature (Lobkis and Weaver, 2001; Derode et al., 2003; Wapenaar, 2004; Wapenaar et al., 2005; Wapenaar et al., 2008; Schuster, 2009). Pioneering work dates back to Aki (1957) who extracted the velocity of the shallow sub-surface from microseismic noise and also to Claerbout (1968) who showed that the autocorrelation of the transmission response is equal to the reflection response and gave its time-reversed version in a layered medium. More recently seismic interferometry was applied in exploration seismology by Bakulin and Calvert (2006) and Schuster et al. (2004), in ultrasound by Weaver and Lobkis (2001), in crustal seismology by Campillo and Paul (2003), Sabra et al. (2005a, b), Roux et al. (2005) and Shapiro et al. (2005), and in helioseismology by Rickett and Claerbout (1999).

Here we investigate the extraction of Green's function based on the cross-correlation of signals at two receivers using seismic energy from a distribution of surrounding sources with a uniform angular spectrum of incident seismic energy. For simplicity we only investigate the acoustic case. Gaussian beams are then used to evaluate the resulting interference integral in order to concentrate the amplitudes of the contributions to a vicinity of the stationary phase directions. This results in a stable estimate, and also provides physical insight into where the dominant contributions of the seismic energy come from in the evaluation of Green's function.

2 Reciprocity of the convolution and correlation types

A derivation of the acoustic reciprocity relations for the convolution and correlation types is now given (see also, Schuster, 2009). In the frequency domain, one can write

$$G(B,A)-G_0(A,B)=$$
$$\int \mathrm{d}S(x)\left[G_0(x,B)\frac{\partial G(x,A)}{\partial n}-G(x,A)\frac{\partial G_0(x,B)}{\partial n}\right], \quad (1)$$

where $G(B, A)$ is the Green's function with a source at A and a receiver at B, and G_0 is a second Green's function for a possibly different medium in the same volume. The integral is along the boundary $\mathrm{d}S(x)$ of the volume. If the

* **Received** 19 April 2010; **accepted in revised form** 3 August 2010; **published** 10 October 2010.
♣ **Corresponding author. e-mail**: nowack@purdue.edu

boundary conditions are homogeneous, the boundary integral vanishes. This could result, for example, if the integration surface is at infinity with Sommerfeld outgoing radiation conditions. If the boundary integral vanishes, and using the same medium for G and G_0, then formal reciprocity of the Green's function results with $G(B, A) = G(A, B)$.

In equation (1), if $G_0(A, B) = G^*(A, B)$, the adjoint Green's function, then

$$G(B, A) - G^*(A, B) = \int \mathrm{d}S(x)\left[G^*(x, B)\frac{\partial G(x, A)}{\partial n} - G(x, A)\frac{\partial G^*(x, B)}{\partial n}\right]. \quad (2)$$

For this case the boundary integral generally does not vanish at infinity. Applying reciprocity of the Green's function then

$$G(B, A) - G^*(B, A) = \int \mathrm{d}S(x)\left[G^*(B, x)\frac{\partial G(A, x)}{\partial n} - G(A, x)\frac{\partial G^*(B, x)}{\partial n}\right]. \quad (3)$$

This is the acoustic reciprocity relation of the correlation type. If the sources at x along the boundary are in the far-field from the receivers, then $\partial G(B, x)/\partial n = \mathrm{i}kG(B, x)$, where $k=\omega/v$ is the wavenumber and v is the velocity. This can then be written as

$$2\mathrm{i}\,\mathrm{Im}G(B, A) = G(B, A) - G^*(B, A) = 2\mathrm{i}k\int \mathrm{d}S(x) G^*(B, x)G(A, x). \quad (4)$$

For this case, we can obtain the imaginary part of the Green's function from B to A from the cross-correlation at the receivers and then integrate over all sources along the boundary. The complete Green's function can then be obtained from this based on the causality properties of the Green's function.

If the sources along the boundary are variable in source strength, a bias in the results could occur, for example, if there are noise sources from distant storms at sea that are dominantly at a small number of locations. However, this can be corrected for if the source strengths along the boundary are known. More generally, the sources along the boundary can have source spectra that are not flat with frequency. In this case, the correlation integral can be written as

$$2\mathrm{i}\,\mathrm{Im}G(B, A) = G(B, A) - G^*(B, A) = 2\mathrm{i}k\int \mathrm{d}S(x)\frac{1}{s_0^2(x, \omega)} P^*(B, x, \omega)P(A, x, \omega), \quad (5)$$

where $P^*(B, x, \omega)$ and $P(A, x, \omega)$ are the general signals from sources on the surrounding boundary each with source spectra $s_0(x, \omega)$ where ω dependence is explicitly shown. Thus, the source spectra, including variable source amplitudes, can be corrected for by dividing out the power-spectra of the sources. However, only the power-spectra are required, or the autocorrelation of the source wavelets, and not the complete source spectra which is a much weaker constraint. For any zeroes in the source spectra, appropriate damping would need to be used.

3 Correlation integral in 2D homogeneous media

In 2D homogeneous media, the Green's function can be written as

$$G(x, x_0) = \frac{\mathrm{i}}{4}\mathrm{H}_0^{(1)}(kr), \quad (6)$$

where $\mathrm{H}_0^{(1)}(kr)$ is a Hankel function, $r=|x-x_0|$ and k is the wavenumber. In the far-field, this can be approximately evaluated as

$$G(x, x_0) = \sqrt{\frac{1}{8\pi kr}}\mathrm{e}^{\mathrm{i}(kr+\pi/4)}. \quad (7)$$

Inserting equation (7) into equation (4) results in (Fan and Snieder, 2009)

$$2\mathrm{i}\,\mathrm{Im}G(B, A) = G(B, A) - G^*(B, A) = \frac{\mathrm{i}}{4\pi}\int \mathrm{d}S(x)\sqrt{\frac{1}{r_{Ax}r_{Bx}}}\mathrm{e}^{\mathrm{i}k(r_{Ax}-r_{Bx})}, \quad (8)$$

where r_{Ax} and r_{Bx} are the distances from x to the receivers A and B, respectively.

If the distance R in Figure 1 is much larger than the distance L between the receivers A and B, then as a first approximation, $r_{Ax} - r_{Bx} = L\cos\phi$ in the exponential and $r_{Ax} = r_{Bx} = R$ in the amplitude term. Letting the arc-length on the circular boundary be $\mathrm{d}S = R\mathrm{d}\phi$, then

$$2\mathrm{i}\,\mathrm{Im}G(B, A) = G(B, A) - G^*(B, A) = \frac{\mathrm{i}}{4\pi}\int \mathrm{d}\phi \exp(\mathrm{i}kL\cos\phi). \quad (9)$$

This results in a plane-wave decomposition of the correlation field from the distant sources at the two receiver positions, and can be represented as a Bessel function, $\mathrm{J}_0(kL)$, where

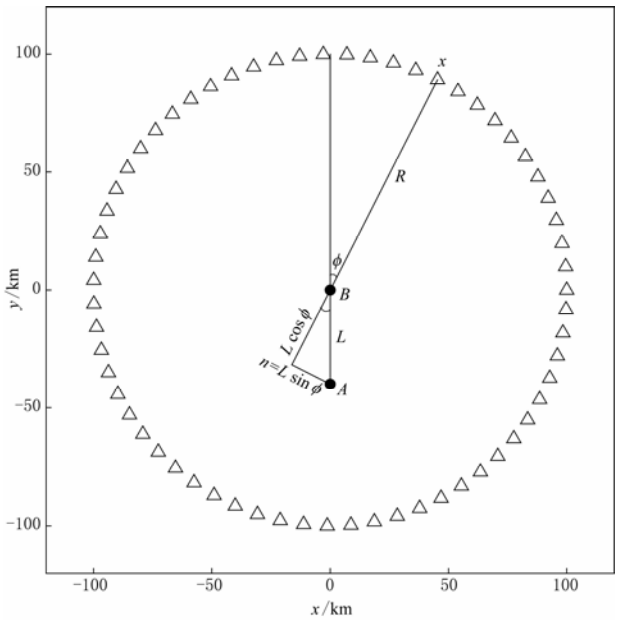

Figure 1 Geometry for the passive estimation of the Green's function between two receivers at *A* and *B* with sources on the surrounding boundary shown by triangles. The distance between the two sensors is *L*. The angle ϕ measures the location along the surrounding circular boundary at a radius *R* from the receiver at *B*.

$$\frac{\mathrm{i}}{2\pi}\int \mathrm{d}\phi \mathrm{e}^{\mathrm{i}kL\cos\phi} = \mathrm{J}_0(kL) = \frac{1}{2}[\mathrm{H}_0^{(1)}(kL) - \mathrm{H}_0^{(1)}(-kL)]. \quad (10)$$

This shows that the correlation Green's function can be written as a sum of plane waves incident on the receivers from distant sources at all angles (Fan and Snieder, 2009).

4 Correlation integral evaluated with Gaussian beams

A paraxial approximation for the phase term in the correlation integral equation (8) can be written as

$$r_{Ax} - r_{Bx} = L\cos\phi + \frac{1}{2}Mn^2, \quad (11)$$

where $L\cos\phi$ is shown in Figure 1, $n = L\sin\phi$, and M is the second derivative of the travel-times at the receiver position A. M is proportional to the wavefront curvature and can be evaluated using dynamic ray tracing, but in a homogeneous medium is known in closed form.

M can now be extrapolated to a complex value where $M=p/q=v^{-1}/(L\cos\phi+\varepsilon)$. ε is called the beam parameter and can be written as $\varepsilon = -\mathrm{i}L_0^2$. The parameter L_0 can be related to the beam-width as $L(s_0)=(2v/\omega)^{1/2}L_0$, where ω is the frequency and v is the medium velocity (see Cerveny et al., 1982; Popov, 1982; Nowack and Aki, 1984). For more recent overviews of Gaussian beam summations, see Cerveny (2001), Popov (2002), Nowack (2003) and Cerveny et al. (2007). The correlation integral with complex beam parameters can then be written as

$$G(B, A) - G^*(B, A) =$$
$$\frac{\mathrm{i}}{4\pi}\int \mathrm{d}\phi \sqrt{\frac{R}{(R + L\cos\phi + \varepsilon)}}\mathrm{e}^{\mathrm{i}\omega(\frac{L\cos\phi}{v}+\frac{1}{2}\mathrm{Re}Mn^2)}\mathrm{e}^{-\frac{\omega}{2}\mathrm{Im}Mn^2}. \quad (12)$$

This results in an amplitude decay instead of just phase interference of the plane wave components in equation (9).

5 Examples

Figure 2 shows results of the correlation integral in equation (9) for the case of the sources on a distant circular boundary where $R = 400$ km with the distance between the two receivers of $L = 10$ km with the geometry shown in Figure 1. The medium velocity is 5 km/s. Sources are positioned every 5 degrees on the circular boundary. However, for plotting purposes in Figure 2 and later plots, a correlation trace is shown every 12 degrees. The waves are assumed to be planar at the receiver locations resulting in the plane-wave decomposition of the correlation integral in equation (9). In order to

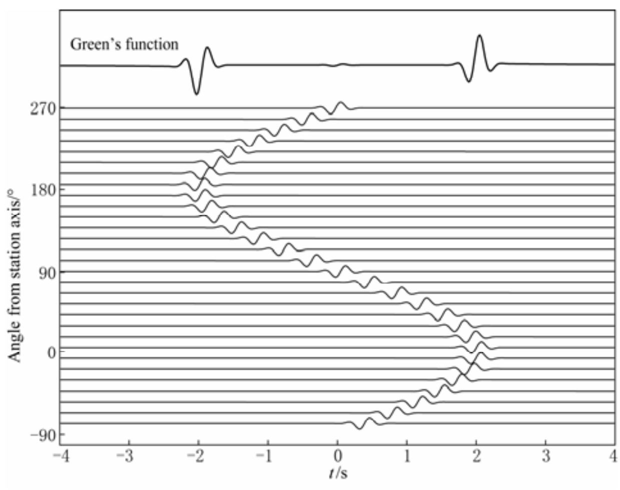

Figure 2 Reconstruction of the Green's function on the top trace from the summation of the integrand components in the correlation integral in equation (4) at the receivers *A* and *B* from the sources as a function of angle on the surrounding circle in Figure 1. A Gabor wavelet is assumed for the source wavelet. Sources are placed every 0.5 degrees on the surrounding circular boundary. However, for plotting purposes only traces every 12 degrees are shown.

investigate a time-domain beam solution for the correlation integral, a Gabor wavelet is used for the sources on the surrounding boundary, and this can be written as

$$f(t) = \exp\left[-\left(2\pi f_M \frac{t-t_i}{\gamma}\right)^2\right]\cos[2\pi f_M (t-t_i)+\nu], \quad (13)$$

where f_M is the center frequency and γ determines the number of wave cycles under the Gaussian envelope (Cerveny, 2001). For the examples shown, f_M=3 Hz, γ=3.5 and ν=0. Thus, the results would be as in equation (9) but convolved with a Gabor wavelet.

For the example shown in Figure 2, the source strengths and source waveforms are the same for all positions on the boundary. The individual components of the integrand are seen to form an inverted S shape as a function of angle. The summation of all the integrand components results in an estimate of the correlation Green's function filtered by the Gabor wavelet and is shown in the top trace. For this case, each of the angular components of the integrand are roughly the same in amplitude and pulse shape, but are located at different times. Nonetheless, the dominant components of the integrand are from angles 0 degree and 180 degrees aligned with the orientation of the two receivers. For these angles, the nearby integrand components are in-phase and provide the dominant stationary phase contributions to the integrand. Components at other angles destructively interfere resulting in no contributions to the correlation integral, with the exception of small end effects at angles of −90 degrees and 270 degrees where the integration terminates.

The regions of stationary phase in the correlation integral are illustrated in Figure 3. The dashed lines show the zones of dominant contributions to the integral based on the stationary phase of the components oriented in the forward and backward directions of the aligned receiver pair. The positive contribution to the correlation Green's function comes from the 0 degree direction, and the negative component from the 180 degree direction. Nonetheless, all components are needed to avoid truncation effects and allow these components to sum to zero by destructive interference. For this case in Figure 2, the source strength is the same for all angular directions on the boundary and results in equal amplitudes of the negative and positive times for the correlation Green's function. However, in the general case, the source strengths will be different, and if not corrected for it will result in different positive and negative time amplitudes for the correlation Green's function.

We would now like to incorporate amplitude weighting of the integrand components using Gaussian beams as described above to assist in concentrating the integrand contributions to near the stationary directions. This also has the advantage of not requiring integration contributions for all angular directions which otherwise would require phase interference, but rather only include those contributions only near the stationary phase directions.

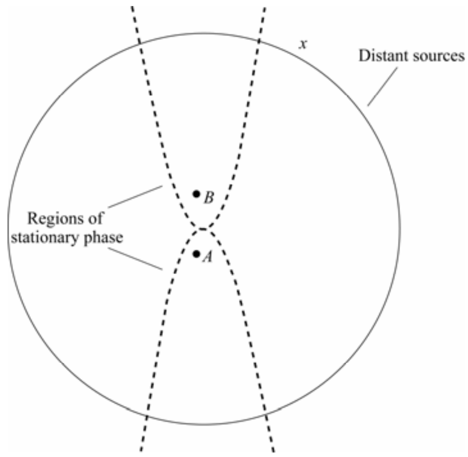

Figure 3 Regions of stationary phase of the oscillatory correlation integral in equation (4) shown by the dashed lines. *A* and *B* are the receiver positions and the sources are located on the circular boundary (modified from Fan and Snieder, 2009).

In Figure 4, the estimate of the correlation Green's function is shown at the top for the case of summation of Gaussian beam correlation components. The geometry of the sources and the two receivers *A* and *B* is again shown in Figure 1. Similar to the plane-wave case, a Gabor wavelet with a reference frequency of 3 Hz is used with equal source amplitudes for all directions on the boundary. For this case, the beam parameter is chosen with L_0=9 which corresponds to a beam-width at the reference frequency of 6.6 km at the receiver *B* location. The use of Gaussian beams can be seen in Figure 4 to restrict the contributions to the vicinity of the stationary phase directions. Also, endpoint errors are removed by the amplitude decay of the beams away from the stationary phase directions. This provides a more stable evaluation of the correlation integral than purely phase interference while also restricting the contributions to just those in the forward and back azimuth directions from the direction of the receiver pair.

The energy in the integrand of the correlation integral can be further concentrated near the stationary phase directions by choosing a smaller beam parameter with L_0=6 which corresponds to a beam-width at the receiver B location of 4.4 km at the reference frequency of the Gabor wavelet. This is shown in Figure 5 where now the concentration of the integrand components of the correlation integral is made smaller still. However, this process can not be taken too far since after a certain point, the beams start to diverge again. An optimally narrow beam-width at the receiver point for planar beams at the initial point was given by Cerveny et al. (1982). Nonetheless, the beam contributions to the correlation integral can be restricted to the first Fresnel zone of the in-phase contributions near the stationary phase directions by a suitable choice of the beam parameter. The sources from other directions are then not required to evaluate the correlation integral using Gaussian beams.

If the source strengths are different but smoothly varying as a function of azimuth, then the stationary phase directions will still be the dominant contributions. However, now there may be differences in the amplitudes for the positive and negative time components of the correlation Green's function. As an example, Figure 6 shows a case that the source strengths vary as $(1+\rho\cos\phi)$ where $\rho=0.3$. In this case, the source strengths in the forward and backward directions vary from 1.3 to 0.7, respectively. This results in an amplitude difference for the positive and negative time components of the correlation Green's function as shown in Figure 6. However, using Gaussian beams for the evaluation of the Green's function clearly identifies where the differences in source strength are coming from.

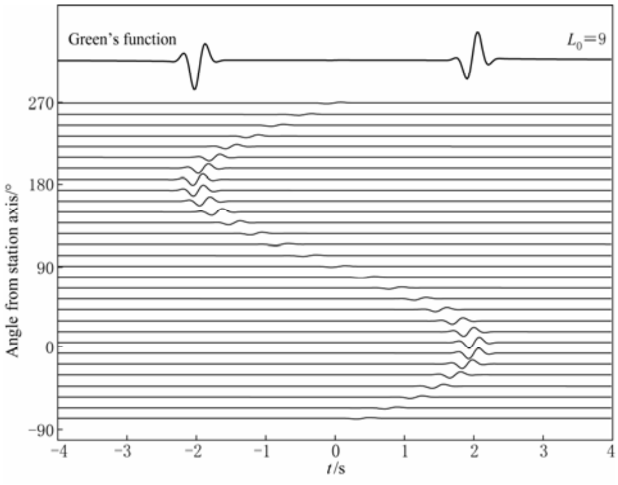

Figure 4 Reconstruction of the Green's function on the top trace from the summation of the integrand Gaussian beam components in the approximate Gaussian beam correlation integral in equation (12). The value L_0 in the complex beam parameter was chosen as 9. A Gabor wavelet is assumed for the source wavelet.

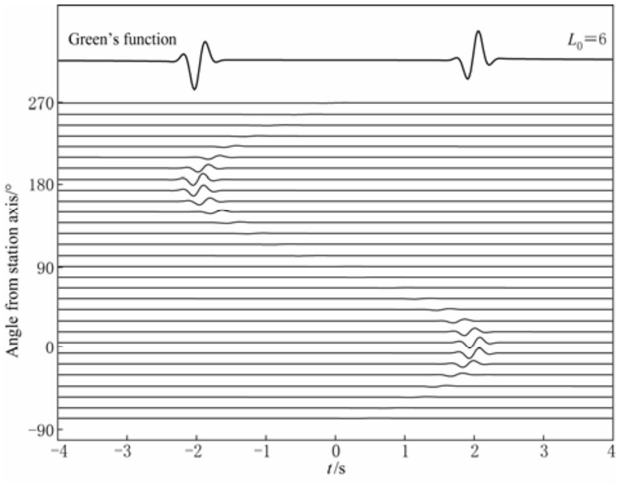

Figure 5 Reconstruction of the Green's function on the top trace from the summation of the integrand Gaussian beam components in the approximate Gaussian beam correlation integral in equation (12). The value L_0 in the complex beam parameter was chosen as 6. A Gabor wavelet is assumed for the source wavelet.

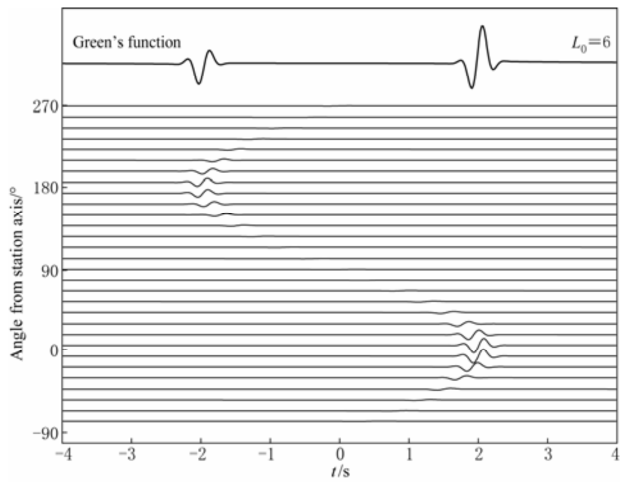

Figure 6 Reconstruction of the Green's function on the top trace from the summation of the integrand Gaussian beam components in the approximate Gaussian beam correlation integral in equation (12). The value L_0 in the complex beam parameter was chosen as 6. A Gabor wavelet is assumed for the source wavelet. For this case, the source strengths were variable as a function of azimuthal angle from the sources and then results in a different amplitude of the summation for the positive times and the negative times.

6 Discussion and conclusions

For the estimation of the Green's function with observed data from controlled sources as in exploration applications, an interferometry formulation similar to equation (5) can be implemented for re-dataming, where $s_0^2(x, \omega)$ are the directionally variable source power-spectra. For observed data from natural noise sources, the signals recorded at each receiver will be a summation from all the sources. However, if the sources are spatially uncorrelated, a formulation similar to equation (5) can also be obtained. For the evaluation of equation (5), the source power-spectra $s_0^2(x, \omega)$ need to be smoothly varying in direction and also nonzero along the stationary phase directions.

For the case of natural noise sources, if the source power spectra are the same for all sources and the noise sources are spatially uncorrelated, then

$$G(B, A) - G^*(B, A) = \frac{2\mathrm{i}k}{s_0^2(\omega)} \left\langle P^*(B, \omega) P(A, \omega) \right\rangle, \quad (14)$$

where the bracket indicates an ensemble average and the $P(A, \omega)$ and $P(B, \omega)$ are the signals recorded at each receiver from all sources (Snieder et al., 2009). The individual or average source terms can be compensated using a deconvolution approach (Snieder et al., 2009) or by using a coherency approach, where

$$G(B, A) - G^*(B, A) = 2\mathrm{i}k \left\langle \frac{P^*(B, \omega) P(A, \omega)}{|P(B, \omega)|\,|P(A, \omega)|} \right\rangle \quad (15)$$

which as noted by Prieto et al. (2009) is analogous to pre-whitening prior to cross-correlation used in many studies (Bensen et al., 2007).

Since the estimated Green's function is often not symmetric with different positive and negative time components, this can be used to infer that equipartition has not been reached resulting from a directional variability of either the density or strength of the sources. This has been utilized by Stehly et al. (2006), Yang and Ritzwoller (2008), Yao et al. (2009) and others with seismic array data to identify the dominant directions of the noise sources. Yao and van der Hilst (2009) used a seismic array in SE Tibet to estimate the non-isotropic distribution of ambient noise energy. They found that the bias from an uneven distribution of noise sources on phase velocities can be suppressed, but will have only a minor effect on the isotropic part of estimated phase velocities. Weaver et al. (2009) estimated corrections for the apparent travel-time of scalar ballistic waves from non-isotropically distributed sources, but found that the effect is small.

A number of researchers have utilized general beam-forming techniques using array data (e.g., Rost and Thomas, 2002) to determine sources of seismic noise, including noise from the oceans and along the coasts (e.g., Roux et al., 2005; Gerstoft et al., 2006; Gerstoft and Tanimoto, 2007; Koper et al., 2009). Also, slant-stacks, the spatial autocorrelation method (SPAC) and other beam-forming methods have been utilized for the analysis of ambient noise recordings in shallow geophysics experiments (Gouedard et al., 2008). In seismic exploration, seismic array data can be used to separate the wavefield data into up- and down-going waves for improvements of the virtual source method (Mehta et al., 2007). Thus for seismic array data, beam-forming can be utilized to decompose the wavefield data into individual components and these can be used for interferometry as in equation (5).

Kimman and Trampert (2010) investigated the effects of non-isotropic source distribution and confirmed the results of Snieder (2004) that interferometry depends on an adequate distribution of sources in the zone of stationary phase along the forward and back directions of the station pair. They then gave an expression from Larose (2005) for the angular size of the interferometric zone of stationary phase as

$$\boldsymbol{\Phi} = \pm\sqrt{\frac{\lambda}{3L}} \quad (16)$$

assuming that the phase differs by less than $\pi/3$, where λ is the dominant wavelength and L is the station separation. However, in their numerical tests they found that this underestimates the angle of necessary coverage by about a factor of 2. Kimman and Trampert (2010) also infer that only including sources in the zone of stationary phase can improve convergence. For example, Roux et al. (2005) just used station pairs in the directions of the largest noise sources for the detection of P-waves.

For the examples shown in Figures 2 and 4–6, the size of the zone of stationary phase at the dominant pulse frequency of 3 Hz is estimated using equation (16) to be $\boldsymbol{\Phi}=\pm 13.5°$. The sources used for these figures are located every 0.5 degrees, but for plotting purposes the correlation traces are plotted every 12 degrees. Thus, from equation (16), the zone of stationary phase would include approximately three correlation traces, 12 degrees apart near the stationary directions, which is approximately consistent with the plots.

The Gaussian beam evaluation of the interferometry integral will self-consistently taper the amplitudes away from the stationary phase directions, and the size of the region of larger Gaussian beam amplitudes will depend on the beam-widths specified, but not smaller than the region of stationary phase. A Gaussian beam summation can be implemented to dynamically utilize only those sources with angles in the vicinity of the stationary points, and will result in more stable evaluations of interferometry integrals. The down-weighting of contributions away from the stationary phase directions will also decrease unwanted noise. In addition, for a limited aperture of sources such as in controlled source experiments, the Gaussian beam decay will reduce unphysical edge effects from a finite source aperture. However, the regions of stationary phase need to be adequately sampled with sources to avoid bias (e.g., Mehta et al., 2008; Yao et al., 2009; Kimman and Trampert, 2010).

In this study, seismic interferometry is investigated for two receivers with sources along the surrounding boundary. The Green's function can then be estimated between the two receivers by the cross-correlation of the signals recorded at both receivers and integrated for all sources. For smoothly varying source strengths with direction, the dominant contribution for the correlation integral is from the stationary phase directions in the forward and back directions from the alignment of the two receivers. The use of Gaussian beams can be used to concentrate the amplitudes of the source contributions to a vicinity of the stationary phase regions, resulting in stable estimates of the Green's function. Several numerical examples are shown to illustrate this process. The application of Gaussian beams to the evaluation of the correlation Green's function provides further insight into how seismic interferometry works.

Acknowledgments The study was supported by U.S. National Science Foundation EAR06-35611 and U.S. Air Force contract FA8718-08-C-002 and partly by the members of the Geo-Mathematical Imaging Group (GMIG) at Purdue University.

References

Aki K (1957). Space and time spectra of stationary stochastic waves with special reference to microtremors. *Bull Earthquake Res Inst* **35**: 415–456.

Bakulin A and Calvert R (2006). The virtual source method: theory and case study. *Geophysics* **71**: SI139–SI150.

Bensen G, Ritzwoller M H, Barmin M P, Levshin A L, Lin F, Moschetti M P, Shapiro N M and Yang Y (2007). Processing seismic ambient noise data to obtain reliable broadband surface wave dispersion measurements. *Geophys J Int* **169**: 1 239–1 260.

Campillo M and Paul A (2003). Long-range correlations in the diffuse seismic coda. *Science* **299**: 547–549.

Cerveny V (2001). *Seismic Ray Theory*. Cambridge University Press, Cambridge, 713 pp.

Cerveny V, Klimes L and Psencík I (2007). Seismic ray theory: Recent developments. *Advances in Geophysics* **48**: 1–126.

Cerveny V, Popov M M and Psencík I (1982). Computation of wavefields in inhomogeneous media — Gaussian beam approach. *Geophys J R astr Soc* **70**: 109–128.

Claerbout J F (1968). Synthesis of a layered medium from its acoustic transmission response. *Geophysics* **33**: 264–269.

Derode A, Larose E, Tanter M, de Rosny J, Tourin A, Campillo M and Fink M (2003). Recovering the Green's function from field-field correlations in an open scattering medium. *J Acoust Soc Am* **113**: 2 973–2 976.

Fan Y and Snieder R (2009). Required source distribution for interferometry of waves and diffusive fields. *Geophys J Int* **179**: 1 232–1 244.

Gerstoft P and Tanimoto T (2007). A year of micoseisms in southern California. *Geophys Res Lett* **34**: L20304, doi:10.1029/2007Gl031091.

Gerstoft P, Fehler M C and Sabra K G (2006). When Katrina hit California. *Geophys Res Lett* **33**: L17308, doi:10.1029/2006 GL027270.

Gouedard P, Cornou C and Roux P (2008). Phase-velocity dispersion curves and small-scale geophysics using noise correlation slantstack technique. *Geophys J Int* **172**: 971–981.

Kimman W P and Trampert J (2010). Approximations in seismic interferometry and their effects on surface waves. *Geophys J Int* **182**: 461–476.

Koper K D, de Foy B and Benz H (2009). Composition and variation of noise at the Yellowknife seismic array. *J Geophys Res* **114**: B10310, doi:10.1029/2009JB006307.

Larose E (2005). *Multiple Scattering of Seismic Waves and Analogous Ultrasonic Experiment*. PhD thesis, LGIT, l'Universite Joseph Fourier, Grenoble, France, 196 pp.

Lobkis O I and Weaver R L (2001). On the emergence of the Green's function in the correlations of a diffuse field. *J Acoust Soc Am* **110**: 3 011–3 017.

Mehta K, Bakulin A, Sheiman J, Calvert R and Snieder R (2007). Improving the virtual source method by wavefield separation. *Geophysics* **72**: V79–V86.

Mehta K, Snieder R, Calvert R and Sheiman J (2008). Acquisition geometry requirements for generating virtual source data. *The Leading Edge* **27**(5): 620–629.

Nowack R L (2003). Calculation of synthetic seismograms with Gaussian beams. *Pure Appl Geophys* **160**: 487–507.

Nowack R L and Aki K (1984). The two-dimensional Gaussian beam synthetic method: testing and application. *J Geophys Res* **89**: 7 797–7 819.

Popov M M (1982). A new method of computation of wave fields using Gaussian beams. *Wave Motion* **4**: 85–97.

Popov M M (2002). *Ray Theory and Gaussian Beam Method for Geophysicists*. Lecture notes, University of Bahia, Salavdor Brazil, 156 pp.

Prieto G A, Lawrence J F and Beroza G C (2009). Anelastic Earth structure from the coherency of the ambient noise field. *J Geophys Res* **114**: B07303, doi: 10.1029/2008JB006067.

Rickett J and Claerbout J (1999). Acoustic daylight imaging via spectral factorization: helioseismology and reservoir monitoring. *The Leading Edge* **18**: 957–960.

Rost S and Thomas C (2002). Array seismology: methods and applications. *Rev Geophys* **40**(3): 1008, doi:10.1029/2000RG 000100.

Roux P, Sabra K G, Gerstoft P, Kuperman W A and Fehler M (2005). P-waves from cross correlation of seismic noise. *Geophys Res Lett* **32**: L19303, doi:10.1029/2005GL023803.

Roux P, Sabra K G, Kuperman W A and Roux A (2005). Ambient noise cross correlation in free space: theoretical approach. *J Acoust Soc Am* **117**: 79–84.

Sabra K G, Roux P, Gerstoft P, Kuperman W A and Fehler M C (2005a). Extracting time-domain Green's function estimates from ambient seismic noise. *Geophys Res Lett* **32**: L03310.

Sabra K G, Roux P, Gerstoft P, Kuperman W A and Fehler M C (2005b). Surface wave tomography from microseisms in southern California. *Geophys Res Lett* **32**: L14311.

Schuster G T (2009). *Seismic Interferometry*. Cambridge University Press, Cambridge, 260 pp.

Schuster G T, Yu J, Sheng J and Rickett J (2004). Interferometric/daylight seismic imaging. *Geophys J Int* **157**: 838–852.

Shapiro N M, Ritzwoller M H and Benson G D (2005). High-resolution surface-wave tomography from ambient noise. *Science* **307**: L03310.

Snieder R (2004). Extracting the Green's function from the correlation of coda waves: a derivation based on stationary phase. *Phys Rev E* **69**: 046610.

Snieder R, Miyazawa M, Slob E, Vasconcelos I and Wapenaar K (2009). A comparison of strategies for seismic interferometry. *Surv Geophys* **30**: 503–523.

Stehly L, Campillo M and Shapiro N (2006). A study of the seismic noise from its long range correlation properties. *J Geophys Res* **111**: B10306, doi:10.1029/2005JB004237.

Wapenaar K (2004). Retrieving the elastodynamic Green's function of an arbitrary inhomogeneous medium by cross correlation. *Phys Res Lett* **93**: 254301.

Wapenaar K, Draganov D and Robertsson J O A eds (2008). *Seismic Interferometry*: *History and Present Status*. Society of Exploration Geophysicists (SEG), Tulsa OK, 628 pp.

Wapenaar K, Fokkema J and Snieder R (2005). Retrieving the Green's function by cross-correlation: A comparison of approaches. *J Acoust Soc Am* **118**: 2 783–2 786.

Weaver R and Lobkis O I (2001). Ultrasonics without a source Thermal fluctuation correlations at MHz frequencies. *Phys Rev Lett* **87**: 134301.

Weaver R, Froment B and Campillo M (2009). On the correlation of non-isotropically distributed ballistic scalar diffuse waves. *J Acoust Soc Am* **126**: 1 817–1 826.

Yang Y and Ritzwoller M H (2008). Characteristics of ambient noise as a source for surface wave tomography. *Geochem Geophys Geosyst* **9**: Q02008, doi:10.1029/2007GC001814.

Yao H and van der Hilst R (2009). Analysis of ambient noise energy distribution and phase velocity bias in ambient noise tomography with application to SE Tibet. *Geophys J Int* **179**: 1 113–1 132.

Yao H, Campman X, de Hoop M V and van der Hilst R (2009). Estimation of surface wave Green's functions from correlation of direct waves, coda waves and ambient noise in SE Tibet. *Phys Earth Planet Int* **177**: 1–11.